

Multi-photon Nonlinear Fluorescence Emission in Upconversion Nanoparticles for Super-Resolution Imaging

by Chaohao CHEN

Thesis submitted in fulfilment of the requirements for
the degree of

Doctor of Philosophy

under the supervision of Dr. Fan Wang, Prof. Dayong Jin,
Dr. Qian Peter Su, Dr. Peter Reece

University of Technology Sydney
Faculty of Science

04/09/2020

Certificate of Original Authorship

I, Chaohao CHEN declare that this thesis is submitted in fulfilment of the requirements for the award of Doctor of Philosophy, in the School of Mathematical and Physical Sciences, Faculty of Science, at the University of Technology Sydney.

This thesis is wholly my own work unless otherwise reference or acknowledged. In addition, I certify that all information sources and literature used are indicated in the thesis.

This document has not been submitted for qualifications at any other academic institution.

This research is supported by the Australian Government Research Training Program.

Production Note:

Signature: Signature removed prior to publication.

Date: 04/09/2020

For my lover

Rui Zhao

Acknowledgements

First and foremost, I would like to express my deep and sincere gratitude to my supervisors. I am particularly grateful to Prof. Jin for offering the opportunity to pursue a PhD in such a great research platform, to Dr Wang for the patient advises and guidances in the experiment designs and modelling simulations, to Dr Su for mentoring the knowledge in biological engineering and Dr Peter Reece in the optical engineering. I would like to thank each of them for their constructive criticisms and helpful discussions on my PhD thesis. Their research attitudes always inspire me to work happily and professionally.

I would like to address a special thanks to Mr Baolei Liu for help developing the image process algorithm, Mr Xuchen Shan for the Labview code and Mr Yongtao Liu for the help of energy level simulations. I would like to acknowledge to Mrs Xiangjun Di, Mr Dejiang Wang and Mr Baoming Wang for their help with cell culture that involved in this thesis. I would also like to thank Dr Jiayan Liao and Dr Shihui Wen for the high-quality upconversion nanoparticle synthesis.

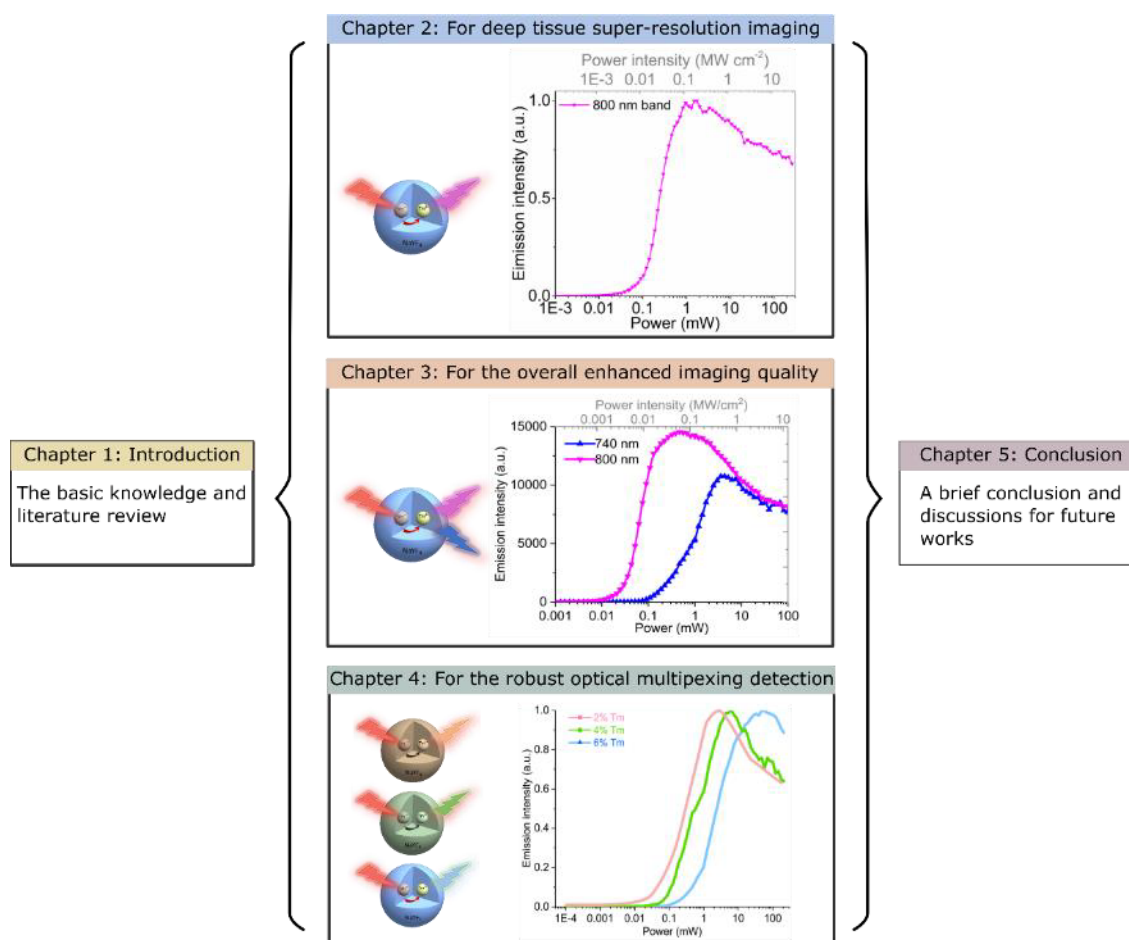
I would like to mention all the member of the IBMD (past and present), who has provided technical supports or experiments suggestions and assistance. I enjoy working with these lovely people and appreciate their help whenever I get any experimental difficulties. I would like to thank all of the friends I have who exist outside the realm of research during the three years in Sydney. Thanks for being so understanding and always keeping my feet on the ground.

I would like to thank my supportive family for their continuous supports and love throughout my whole life. Specially thanks to my wife Rui Zhao, for her understanding and incalculable contribution to our little family.

Finally, I would like to acknowledge the Australian Government Research Training Program and the China Scholarship Council Scholarship for providing the scholarship and research opportunities.

Format of Thesis

This thesis consists of five chapters. Chapter 1 is the introduction and in Chapters 2-4 the research results are the focus on applying optical nonlinear response curves of upconversion nanoparticles. The objective is to implement new modalities of super-resolution microscopies. Chapter 5 concludes this thesis with a summation of the main themes covered in this investigation. This thesis flowchart is illustrated below.



This thesis summarizes the key results from my PhD research program, in which the topic covered is super-resolution microscopy and nanoparticle-based super-resolution microscopy. My PhD sets out to develop new super-resolution microscopy methods using advanced nanomaterials. The main bulk of the framework developed for this thesis consists of three results chapters. The first chapter describes the use of a near-infrared nonlinear response curve from a single nanoparticle to develop a deep tissue super-resolution imaging method. The second results chapter takes advantages of the two response curves from two emission bands of a single nanoparticle, which yields two

things: the overall improved image quality; and increased imaging speed. In the third chapter concerning the results, I explore the multiple emission curves derived from different nanoparticles for robust optical multiplexing detection. Lastly, the conclusion and discussions for future research are provided.

List of Publications

➤ Articles

1. **Chen, C.**, Liu, B., Liu, Y., Liao, J., Wang, F. & Jin, D. Fourier domain heterochromatic fusion for single beam scanning super-resolution microscopy. (Under revision)
2. **Chen, C.**[†], Wang, F.[†], ... & Jin, D. Multi-photon near-infrared emission saturation nanoscopy using upconversion nanoparticles. *Nature Communications* (2018), 9:3290.
3. **Chen, C.**, Liu, Z. & Jin, D. Bypassing the limit in volumetric imaging of mesoscale specimens. *Advanced Photonics* (2019) 1.2 : 020502.
4. Liu, B., **Chen, C.**, Di, X., Wang, F. & Jin, D. Upconversion nonlinear structured illumination microscopy. *Nano Letter* (2020) 20, 7, 4775-4781.
5. Liao, J., Jin, D, **Chen, C.**, Li, Y. & Zhou, J. Helix shape power-dependent properties of single upconversion nanoparticles. *Journal of Physical Chemistry Letters* (2020) 11, 8, 2883-2890.
6. Liu, Y., Wang, F., Liu, H., Fang, G., Wen., **Chen, C.** ... & Jin, D. Super-Resolution Mapping of Single Nanoparticles inside Tumor Spheroids. *Small* (2020) 10.1002. 201905572.
7. Clarke, C., Liu, D., Wang, F., Liu, Y., **Chen, C.**, ... & Jin, D. Large-scale dewetting assembly of gold nanoparticles for plasmonic enhanced upconversion nanoparticles. *Nanoscale* (2018) 10 (14), 6270-6276.

➤ Publication in the conference proceeding

8. **Chen, C.**, Wang, F.... & Jin, D. Upconversion nanoparticles assisted multi-photon fluorescence saturation microscopy. In Nanoscale Imaging, Sensing, and Actuation for Biomedical Applications XVI (Vol. 10891, p. 108910S). International Society for Optics and Photonics. SPIE 2019

➤ Patents

9. Wang, F., Jin, D. & **Chen, C.** A super-resolution imaging method, a plurality of upconversion nanoparticle fluorophores, and a super-resolution scanning microscope. WO2020028942A1, 2020-02-13. WIPO (PCT)
10. **Chen, C.**, Jin, D. & Wang, F. A super-resolution imaging method, a plurality of upconversion nanoparticle fluorophores, and a super-resolution scanning microscope. AU2018902855A0, 2018-08-16, (Australian Patent)

([1,2,8,9,10] are closely related to my PhD program)

Table of Symbols

λ	Acoustic radiation force	α	Objective aperture angle
n	Refractive index	I_{max}	Maximum STED beam power
I_{sat}	Saturation intensity	$h\nu$	Photon energy
σ	Cross-section of excitation	τ_{fl}	Fluorescence lifetime
T_1	The metastable dark triplet state	N	Total captured number of photons
s	The standard deviation of Gaussian function	b	The standard deviation of the background noise
I_{FED}	Image of FED	I_{Gau}	Image of a Gaussian beam
I_{Dou}	Image of a doughnut beam	r	A normalising coefficient
R_{tr}	The transmission ratio	P	The beam power
r_o	The loss rate of the objective lens	t_τ	The exposure time
A	The area of the focused laser spot	f	The pulse frequency
t_p	The pulse duration	α_λ	The attenuation coefficient
l	The path length	h_o	The FWHM of confocal PSF
ς	The saturation factor	k_{BA}	The carrier transition rate
σ_{TPA}	The molecular cross-section	$h_{em}(x)$	PSF of emission
$h_{exc}(x)$	PSF of the excitation beam	η	Emission response curve
$h_c(x)$	PSF of the confocal system	PSF_{Gau}	Gaussian PSF
PSF_{Dou}	Doughnut PSF	OTF_{eff}	Processed effective OTF
I_{eff}	Processed effective image	OTF_{Gau}	Gaussian OTF
OTF_{Dou}	Doughnut OTF		

Abbreviations

UCNPs	upconversion nanoparticles
NIRES	near-infrared emission saturation
PSFs	point speared functions
FWHM	full width at half maximum
SEM	scanning electron microscopy
TEM	transmission electron microscopy
TIRF	total internal reflection fluorecence
SNOM	scanning near-field optical microscopy
RESOLFT	reversible saturable or switchable optical fluorecence transitions
STED	stimulated emission depletion
GSD	ground-state depletion
SIM	structured illumination microscopy
PALM	photoactivated localisation microscopy
STORM	stochastic optical reconstruction microscopy
OTF	optical transfer functions
SPEM	saturated pattern excitation microscopy
SMLM	single-molecule localisation microscopy
FRC	Fourier ring correlation
SOFI	super-resolution optical fluctuation imaging
PAINT	point accumulation for imaging in nanoscale topography
QDots	quantum dots
CDots	carbon dots
PDots	polymer dots
AIE	aggregation-induced emission

UV	ultraviolet
ACQ	aggregation caused quenching
FED	fluorescence emission difference
MPLSM	multi-photon laser scanning microscopy
NIR	near-infrared
CW	continuous-wave
SW	single wavelength
VPP	vortex phase plate
HWP	half-wave plate
PBS	polarised beam splitter
DM	dichroic mirror
QWP	quarter-wave plate
BPF	bandpass filters
MMF	multimode fibre
SPAD	single-photon counting avalanche photodiode
OA	oleic acid
PFA	Paraformaldehyde
DFT	discrete Fourier transform
FFT	fast Fourier transform
THF	tetrahydrofuran
BSA	bovine serum albumin
BSA	bovine serum albumin
ISM	imaging scanning microscopy
LLS	lattice light sheet

Table of Contents

Acknowledgements	i
Format of Thesis	ii
List of Publications	iv
Table of Symbols	v
Abbreviations	vi
List of Figures	xi
List of Tables	xvi
Abstract	xvii
Chapter 1 Introduction	1
1.1 Diffraction limit in microscopy	2
1.2 Super-resolution technology	3
1.2.1 Patterned excitation approach	4
1.2.2 Single-molecule localization	11
1.3 Nanoparticles in super-resolution techniques	17
1.3.1 Quantum dots (QDots)	17
1.3.2 Carbon dots (CDots)	19
1.3.3 Polymer dots (PDots)	21
1.3.4 Aggregation-induced emission (AIE) dots	23
1.3.5 Lanthanide-doped upconversion nanoparticles (UCNPs)	24
1.4 Aim and outline	28
Chapter 2 Multi-photon near-infrared emission saturation nanoscopy for deep tissue imaging by using UCNPs	30
2.1 Background.....	31
2.2 Advantage of UCNPs in deep tissue imaging	34
2.3 Principle of NIRES nanoscopy	36
2.3.1 Photon transition system in UCNPs	36
2.3.2 Saturation effect with the doughnut-shaped beam	39

2.3.3	Emission saturation enabled sub-diffraction resolution.....	40
2.4	Methods.....	43
2.4.1	Experimental setup	43
2.4.2	Materials.....	44
2.4.3	Biological samples.....	48
2.5	Results and discussion.....	50
2.5.1	Optimal emission band.....	50
2.5.2	Resolution dependent on Tm-doped and excitation power.....	51
2.5.3	Resolution improved by Yb-doped and core-shell structure.....	54
2.5.4	Resolving single UCNPs inside HeLa cell	57
2.5.5	Deep tissue imaging by NIRES	58
2.5.6	Discussion.....	61
2.6	Conclusion	62
Chapter 3 Fourier domain heterochromatic fusion for super-resolution microscopy by point-spread-function engineering.....		63
3.1	Background	63
3.2	Spatial frequency domain.....	65
3.2.1	Image spatial frequency and spectrum.....	65
3.2.2	Fourier transform.....	67
3.2.3	Fast Fourier transform	69
3.2.4	Convolution and deconvolution.....	70
3.2.5	Image filtering	72
3.3	The multicolour PSF engineering super-resolution microscopy	75
3.3.1	Image subtraction	76
3.3.2	Fourier fusion	80
3.4	Methods.....	86
3.4.1	Experimental setup	86
3.4.2	Materials.....	87
3.4.3	Cellular immunofluorescence.....	88

3.5	Results and discussion	89
3.5.1	Multicolour emission in UCNPs	89
3.5.2	Fourier fusion on single nanoparticles	93
3.5.3	Comparison of different algorithms	97
3.5.4	Fourier fusion on continuous specimens	99
3.5.5	Evaluating image resolution.....	101
3.5.6	Discussion	104
3.6	Conclusion	106
Chapter 4 Distinct nonlinear optical response encoded single nanoparticle for multiplexed detection		108
4.1	Background.....	108
4.2	The principle of PSF engineering for imaging recognition	110
4.2.1	Adjusting the excitation power by polarization.....	110
4.2.2	Nonlinear response in UCNPs	111
4.2.3	PSF engineering encoding the nonlinear response curves.....	113
4.3	Results and discussion	115
4.3.1	Verifying the PSF engineering by filters.....	115
4.3.2	Classifying multiple UCNPs at the same intensity with the same colour	117
4.3.3	Multiplexing detection of the biomarkers	117
4.3.4	Discussion	118
4.4	Conclusion	119
Chapter 5 Conclusion and Future work.....		120
5.1	Conclusion	120
5.2	Future work	121
5.2.1	Doughnut beam with rare-earth nanocrystals.....	122
5.2.2	Doughnut beam with other fluorescent materials.....	124
Appendix I		125
Appendix II		131
References		137

List of Figures

Figure 1-1 The principle of a STED microscope.	5
Figure 1-2 The principle of a GSD microscope. (a) A simplified energy level of stimulated emission. (b) An energy level illustration of a GSD. S_0 is the ground state, S_1 is the excited state, T_1 is a metastable triplet state.	8
Figure 1-3 The principle of a SIM microscope.	9
Figure 1-4 The principle of an SMLM microscope.	12
Figure 1-5 The principle of a PAINT microscope.	15
Figure 1-6 Immunofluorescence imaging results of with QDots.	18
Figure 1-7 Super-resolution imaging of CDots-labelled structures inside a cell... ..	20
Figure 1-8 Super-resolution nanoscopy of subcellular structures labelled with small photoblinking PDots.	21
Figure 1-9 Super-resolution imaging of the subcellular structures labelled using AIE dots.	23
Figure 1-10 Subdiffraction imaging with UCNPs.....	25
Figure 2-1 Diagram of the conventional two-photon emission.....	31
Figure 2-2 Diagram of upconversion emission in UCNPs.....	33
Figure 2-3 Summary of the minimum energy densities required by a range of optical probes for deep tissue super-resolution imaging.....	36
Figure 2-4 Rate transition system of UNCPs.	37
Figure 2-5 Simulated excitation power-dependent emission intensity.	39
Figure 2-6 Theoretical simulation of the image of single UCNP by NIRES.	40
Figure 2-7 The simplified energy levels and 800 nm emission power dependence of Yb^{3+} and Tm^{3+} co-doped UCNPs.	41
Figure 2-8 The principle of NIRES nanoscopy using UCNP as a multi-photon probe for deep tissue imaging.	41

Figure 2-9 Experimental setup for NIRES nanoscopy.....	43
Figure 2-10 TEM images (left) and size distribution histograms (right) of the nanoparticles.	46
Figure 2-11 The upconversion emission spectra from UCNPs.....	47
Figure 2-12 The saturation intensity curve of the 800 nm emissions from UCNPs.	48
Figure 2-13 Photographs of different mouse tissue slices on glass slides.	49
Figure 2-14 UV–vis absorption spectra of the 50 μm and 100 μm live, brain, and kidney tissue slice samples, respectively.	49
Figure 2-15 Optimal emission band to achieve high resolution under the same excitation power.....	50
Figure 2-16 The acquired images of different Tm^{3+} doping concentration of UCNP (NaYF_4 : 20% Yb^{3+} , $x\%$ Tm^{3+} , ~ 40 nm in diameter) under different excitation power..	51
Figure 2-17 Super-resolution scaling Δr of UCNPs (NaYF_4 : 20% Yb^{3+} , $x\%$ Tm^{3+} , ~ 40 nm in diameter; $x = 2, 3, 4, 6$ and 8) as a function of the excitation power (intensity)..	52
Figure 2-18 Two cross-section line profiles with negative-shaped PSF overlapping with different centre distance from 10 nm to 50 nm.....	53
Figure 2-19 The resolution can be improved by increasing sensitizer concentration...	54
Figure 2-20 The resolution can be improved by adding an inert shell.....	55
Figure 2-21 800 nm emission saturation curves of UCNPs with different size.....	56
Figure 2-22 NIRES super-resolution imaging of single UCNPs inside the HeLa cell.	57
Figure 2-23 Resolved two particles with distance below the diffraction limit.	58
Figure 2-24 The penetration depth of different emission bands and optical resolution of different imaging modalities at different depth of a liver tissue slice.....	59
Figure 2-25 NIRES nanoscopy for super-resolution imaging of single UCNPs through deep mouse liver tissue.	60
Figure 2-26 NIRES images in the deep mouse brain and kidney tissue.	61

Figure 3-1 The line pairs in an image plane.....	66
Figure 3-2 The process of image convolution.....	71
Figure 3-3 Image filtering in the spatial domain.....	72
Figure 3-4 The ideal image filter.....	74
Figure 3-5 The Gaussian image filter.....	75
Figure 3-6 The Butterworth image filter.....	75
Figure 3-7 The concept of multicolour PSF engineering super-resolution microscopy.	76
Figure 3-8 The principle of the FED image subtraction.	77
Figure 3-9 A series of patterns consisted of emitters with varying distances for simulation.	78
Figure 3-10 Simulation result by FED image subtraction.....	79
Figure 3-11 The OTF profiled of the FED image subtraction.	79
Figure 3-12 Schematics of Fourier fusion for super-resolution microscopy..	80
Figure 3-13 Schematics of binary masks for Fourier fusion.....	81
Figure 3-14 Effective PSF for the fusion process by using the Gaussian and doughnut PSF.....	82
Figure 3-15 The flow chart of the Fourier domain heterochromatic fusion method.....	83
Figure 3-16 A numerical study using the heterochromatic Fourier spectrum fusion algorithm to overcome the issues associated with frequency deficiency and imaging distortion.	84
Figure 3-17 The magnified images for the Gaussian, doughnut and Fourier fusion comparison.....	85
Figure 3-18 The OTF for the Gaussian, doughnut and Fourier fusion comparison.....	85
Figure 3-19 Schematic of the single beam Fourier fusion super-resolution nanoscopy.	86
Figure 3-20 The upconversion emission spectra from UCNPs.....	89

Figure 3-21 Heterochromatic emission saturation contrast produced by UCNPs and power-dependent emission PSF patterns under a tightly focused doughnut beam illumination.	90
Figure 3-22 The experimental and theoretical simulation of the process for generating Gaussian PSF under a doughnut beam.	91
Figure 3-23 The cross-section profiles of the simulated PSF at 800 nm emission band under different excitation power.	92
Figure 3-24 The standard confocal images of UCNPs by scanning a standard Gaussian beam.	93
Figure 3-25 The multicolour images of UCNPs by scanning a doughnut-shaped beam.	93
Figure 3-26 Super-resolution imaging of single UCNPs using Fourier fusion.	94
Figure 3-27 The statistic size distribution of the nanoparticles NaYF ₄ : 40% Yb ³⁺ , 4% Tm ³⁺ in TEM and Fourier domain fusion super-resolution imaging.	95
Figure 3-28 Photo-stability tests of UCNPs used in super-resolution microscopy.	95
Figure 3-29 Heterochromatic emission saturation contrast for the low lanthanide-doped UCNPs.	96
Figure 3-30 The sub-diffraction imaging of the lower activator doped UCNPs (2% Tm ³⁺ and 40% Yb ³⁺).	97
Figure 3-31 Comparison of different algorithms.	98
Figure 3-32 Simulated images of the microtubule network.	99
Figure 3-33 Simulation of Fourier domain heterochromatic fusion imaging of cell microtubules.	100
Figure 3-34 Numerical study from Fourier domain heterochromatic fusion imaging of cell microtubules.	100
Figure 3-35 FRC analysis on the imaging quality of Gaussian, doughnut and Fourier fusion PSFs. in Figure 3-33a-c.	101

Figure 3-36 Large-scale super resolution imaging results of the patterned structure using Fourier domain heterochromatic fusion.	102
Figure 3-37 The decorrelation analysis for the image processed by different methods.	104
Figure 3-38 Schematics and optical properties of upconversion nanoparticles for hyperspectrum Fourier domain heterochromatic fusion in single beam scanning super-resolution microscopy.	105
Figure 4-1 The working principle by employing polarization to control the excitation power change.	110
Figure 4-2 Multiplexed detection strategy for imaging two types of UCNPs at the same emission colour band.....	111
Figure 4-3 Confocal microscopy images and statistical intensities of UCNPs.....	112
Figure 4-4 The emission response curves of Tm and Er doped UCNPs.....	112
Figure 4-5 The concept of PSF engineering encoding the nonlinear response curves for nanoparticles recognition.	113
Figure 4-6 The emission features of Tm ³⁺ and Er ³⁺ doped UCNPs.	114
Figure 4-7 Verifying the PSF engineering to classify the single nanoparticles by filters.	115
Figure 4-8 Classifying multiple UCNPs at the same intensity with the same colour.	116
Figure 4-9 Multiplexing detection of the biomarkers.	117
Figure 4-10 The parameters in the emission pattern help to classify different particles accurately.	118
Figure 5-1 Reducing the excitation power for NIREs microscopy using a mirror substrate.	123

List of Tables

Table 2-1 Key parameters of various imaging modalities for deep tissue using nanoparticles.	35
Table 2-2 The values of key constants and rate parameters used in the simulations....	38
Table 2-3 FWHM of 455 nm, 800 nm confocal and NIRES at different depth of a tissue slice.	58

Abstract

Due to the unique optical properties gained by converting near-infrared light to shorter wavelength emissions, upconversion nanoparticles (UCNPs) have attracted considerable interest. Their superior features, including their multi-wavelength emissions, optical uniformity, background suppression, photostability and deep penetration depth through the tissue, make them extremely suitable for biological and biomedical applications. By taking advantage of their multi-photon nonlinear emissions in UCNPs, the goal of this thesis is to develop UCNPs-based super-resolution microscopy methods to address the challenges currently facing nanoscopy, for instance complexity, stability, limited penetration through the tissue and low throughput. The methods being investigated in this thesis make concrete the specific advantages in terms of image depth, speed, overall quality, and multiplexing potentials. To unlock a new mode of deep tissue super-resolution imaging, I first developed the near-infrared emission saturation (NIREs) nanoscopy by taking advantage of near-infrared-in and near-infrared-out optical nonlinear response curve from a single upconversion nanoparticle. This approach only requires two orders of magnitude that are lower than the excitation intensity, which is generally required for conventional multi-photon dyes. This work achieves a super-resolution of sub 50 nm, less than $1/20^{\text{th}}$ of the excitation wavelength, and can image single UCNP through a 93 μm thick liver tissue.

To improve the overall imaging quality and simplify the system setups, I further exploited the distinct nonlinear photon response curves from the two emission bands in UCNP, and explored an opportunity for a tightly focused doughnut excitation to generate distinct spectral dependent point spread functions (PSFs). With controllable PSFs from multi-channel emissions by the excitation power density, this work presents the possibility of achieving super-resolution imaging under saturated fluorescence excitation via PSF engineering. Moreover, I developed a multicolour Fourier fusion algorithm to enlarge the optical system's frequency shifting ability, and yield an enhanced imaging quality at a higher imaging speed. By realising the uniform and distinct nonlinear emission curves from different nanoparticles, this work posits a new optical encoding dimension for multiplexing imaging. Proposed here is a robust PSF engineering strategy to extract emitter properties. This work extends the multiplexing capacity of UCNPs and offers new

opportunities for their applications. These methods are my contributions to the search for a stable, viable, and multifunctional optical imaging modality for the nanoscale context.